

# 1 Exploring the niche concept in a simple metaorganism

2

3

4 Peter Deines<sup>1\*</sup>, Katrin Hammerschmidt<sup>2</sup> and Thomas CG Bosch<sup>1</sup>

5

6 <sup>1</sup>Zoological Institute, Christian-Albrechts-University Kiel, 24118 Kiel, Germany7 <sup>2</sup>Institute of General Microbiology, Christian-Albrechts-University Kiel, 24118 Kiel,  
8 Germany

9

10 \*Correspondence:

11 Peter Deines

12 pdeines@zoologie.uni-kiel.de

13

14

## 15 Abstract

16 Organisms and their resident microbial communities - the microbiome - form a  
17 complex and mostly stable ecosystem. It is known that the specific composition and  
18 abundance of certain bacterial species have a major impact on host health and  
19 *Darwinian fitness*, but the processes that lead to these microbial patterns have not yet  
20 been identified. We here apply the niche concept and trait-based approaches as a first  
21 step in understanding the patterns underlying microbial community assembly and  
22 structure in the simple metaorganism *Hydra*. We find that the carrying capacities in  
23 single associations do not reflect microbiota densities as part of the community,  
24 indicating a discrepancy between the fundamental and realized niche. Whereas in  
25 most cases, the realized niche is smaller than the fundamental one, as predicted by  
26 theory, the opposite is observed for *Hydra*'s two main bacterial colonizers. Both,  
27 *Curvibacter sp.* and *Duganella sp.* benefit from association with the other members of  
28 the microbiome and reach higher fractions as in single colonisations. This cannot be  
29 linked to any particular trait that is relevant for interacting with the host or by the  
30 utilization of specific nutrients but is most likely determined by metabolic interactions  
31 between the individual microbiome members.

32

33

34 Keywords

35 fundamental niche, realized niche, microbiome, species abundance, microbial traits,  
36 *Hydra*

37

38 Running title

39 Microbial traits, niches, and the metaorganism

40

41

42 Number of words: 4590

43 Number of figures: 6

44

45

46

## 47 **Introduction**

48 Microbiomes contribute to ecosystems as key engines that power system-level  
49 processes (Falkowski et al., 2008). This also applies to host ecosystems, where they  
50 are critical in maintaining host health, survival, and function (Kau et al., 2011;  
51 McFall-Ngai et al., 2013). Despite their importance, the mechanisms governing  
52 microbiome assembly and composition are largely unknown. This is different for  
53 macroscopic communities, thanks to the application of niche (Holt, 2009; Leibold,  
54 1995; Whittaker et al., 1973) and trait-based theories, which might also provide a  
55 useful framework for studying the ecology and evolution of microbiomes in  
56 metaorganisms (Kopac and Klassen, 2016).

57 The niche concept is one of the core concepts in ecology and has been  
58 rediscovered by modern ecology for explaining biodiversity and species coexistence  
59 patterns (Pocheville, 2015). The niche-based theory states that an ecological  
60 community is made up of a limited number of niches, each occupied by a single  
61 species. Hutchinson (Hutchinson, 1957) defined the *fundamental niche* as the needs of  
62 a species for it to maintain a positive population growth rate, disregarding biotic  
63 interactions (Hutchinson, 1957; Pearman et al., 2008). The fundamental niche  
64 therefore represents an idealized situation exclusive of interspecific interactions. The  
65 effect of biological interactions is taken into account in the definition of the *realized*  
66 *niche* (Hutchinson, 1957). This is the portion of the fundamental niche in which a  
67 species has a positive population growth rate, despite the constraining effects of  
68 biological interactions, such as inter-specific competition (Hutchinson, 1957;  
69 Pearman et al., 2008).

70 In the last two decades, the shift from taxonomy to function by using trait-  
71 based approaches has provided a detailed understanding of biodiversity-ecosystem  
72 functioning (Louca et al., 2018). Recently, this framework is also being used by  
73 microbial ecologists to study microbial biogeography (Green et al., 2008), or to  
74 unravel microbial biodiversity-ecosystem functioning relationships (Krause et al.,  
75 2014). Further, this approach allows studying microbiomes in the light of coexisting  
76 traits/ functions rather than of coexisting microbes (Martiny et al., 2015). A recent  
77 study successfully used this approach and analysed trait-based patterns to understand  
78 the mechanisms of community assembly and succession of the infant gut microbiome  
79 (Guittar et al., 2019). Microbial traits cover a range of phenotypic characteristics  
80 ranging from simple to complex, for example organic phosphate utilization,  
81 bacteriophage host range, cellulose degradation, biofilm formation, nitrogen fixation,  
82 methanogenesis, and salinity preference (Martiny et al., 2015). Potential microbial  
83 traits can be measured directly by laboratory assays (as in this study) or can be  
84 indirectly inferred based on genomic information.

85 The aim of this study is to apply the niche concept and trait-based theory to  
86 the metaorganism *Hydra* to gain insight into the mechanisms underlying the microbial  
87 community composition. We thus specifically extend the niche-assembly perspective,  
88 classically used for assessing species assembly and coexistence in abiotic  
89 environments, to a host-associated microbiome, thus a biotic environment.

90 The freshwater polyp *Hydra* and its microbiome have become a valuable  
91 model system for metaorganism research as it provides a bridge between the  
92 simplicity of synthetic communities and the complex mouse model (Deines and  
93 Bosch, 2016). The ectoderm is covered by a multi-layered glycocalyx, which is the  
94 habitat for a highly stable species-specific microbiome of low complexity (Bosch,  
95 2013; Deines et al., 2017; Franzenburg et al., 2013). The most abundant bacterial  
96 colonizers of *Hydra vulgaris* (strain AEP) can be cultured and manipulated *in vitro*

97 (Bosch, 2013; Fraune et al., 2015; Wein et al., 2018), allowing the measurement of  
98 phenotypic microbial traits and fitness. Fitness, as defined by niche theory, is the  
99 positive population growth of the focal species, which in our study is that of the six  
100 isolated microbiome members. Measurements of the performance of the bacterial  
101 populations when grown singly, i.e. in the absence of the other microbial competitors  
102 *in vitro* and *in vivo* (on germ-free *Hydra* polys), specify the fundamental niche. For  
103 each species, we compare the fundamental niche to the realized niche, which we  
104 calculated based on published data on the microbiome composition of wild-type and  
105 conventionalized polys (germ-free polys incubated with tissue homogenates of wild-  
106 type animals) (Franzenburg et al., 2013; Murillo-Rincon et al., 2017). We also  
107 measure phenotypic traits that might be connected to the success of the various  
108 microbial species in occupying the fundamental niche; these are essentially traits that  
109 might play a role in successfully populating their environment, the host, such as  
110 biofilm formation, surface hydrophobicity (bacterial cells are more likely to attach to  
111 surfaces with the same hydrophobicity), and nutrient utilisation patterns. As the  
112 realized niche is determined by biological interactions of one species with its  
113 associate microbial community, we focus on traits that are important when competing  
114 with other species, such as growth rate, niche overlap, and niche breadth. Ultimately,  
115 we take the traits and the ecological niches as determinants of species interactions,  
116 which may infer the assembly and structure of the host-associated microbiome.  
117

## 118 **Materials and Methods**

### 119 **Animals used, culture conditions, and generation of germ-free animals**

120 *Hydra vulgaris* (strain AEP) was used in the experiments and cultured according to  
121 standard procedures at 18°C in standardized *Hydra* culture medium (Lenhoff and  
122 Brown, 1970). Animals were fed three times a week with 1st instar larvae of *Artemia*  
123 *salina*. Germ-free polyps were obtained as previously described (Franzenburg et al.,  
124 2013; Murillo-Rincon et al., 2017). After two weeks of treatment, polyps were  
125 transferred into antibiotic-free sterile *Hydra* culture medium for recovery (four days).  
126 Sterility was confirmed by established methods (Franzenburg et al., 2013). During  
127 antibiotic treatment and re-colonization experiments, polyps were not fed.

128

### 129 **Bacterial species and media**

130 The bacterial species used in this study are *Curvibacter* sp. AEP1.3, *Duganella* sp.  
131 C1.2, *Undibacterium* sp. C1.1, *Acidovorax* sp. AEP1.4, *Pseudomonas* sp. C2.2,  
132 *Pelomonas* sp. AEP2.2., which are species isolated from the *Hydra vulgaris* (strain  
133 AEP) microbiome (Fraune et al., 2015). These bacteria were cultured from existing  
134 isolate stocks in R2A medium at 18°C, shaken at 250 r.p.m for 72 h before use in the  
135 different experiments.

136

### 137 **Fundamental and realized niche**

138 Germ-free polyps were inoculated with single bacterial species using  $5 \times 10^3$  cells in 1.5  
139 ml Eppendorf tubes containing 1 ml of sterile *Hydra* culture medium. After 24 h of  
140 incubation, all polyps were washed with, and transferred to sterile *Hydra* culture  
141 medium, incubated at 18°C. After three days of incubation individual polyps were  
142 homogenized in an Eppendorf tube using a sterile pestle, after which serial dilutions  
143 of the homogenate were plated on R2A agar plates to determine colony-forming units  
144 (CFUs) per polyp (Deines et al., 2020).

145 The carrying capacities of mono-associations provide information of the  
146 occupied niche space on the host in the absence of other microbial species that are  
147 part of the microbiome, and thus specifies the fundamental niche for each (as  
148 calculated from the proportion of each species from the sum of all).

149 Estimates of the realized niche are based on underlying original data of previously  
150 published values of community composition and relative abundances (as estimated  
151 based on OTUs) of wild-type and conventionalized polyps that have been reported to  
152 be remarkably stable over time (Bosch, 2013; Franzenburg et al., 2013; Fraune et al.,  
153 2015; Murillo-Rincon et al., 2017).

154 Note that carrying capacities of the members when part of the full community  
155 could not be assessed via plating of the community as was done for the mono-  
156 associations as not all bacterial species can be differentiated based on colony  
157 morphology, which is why we based calculations of the realized niche on data that  
158 was previously published (Franzenburg et al., 2013; Fraune et al., 2015; Murillo-  
159 Rincon et al., 2017). Data from another study (Deines et al., 2020) demonstrates that  
160 germ-free polyps, which were inoculated with the natural community of species  
161 (conventionalized animals), harbour an equally dense microbiome as wild-type  
162 polyps. This indicates that the generation and re-exposure of germ-free animals does  
163 not lead to an overall change in carrying capacity.

164

### 165 **Cell surface hydrophobicity (CSH)**

166 The BATH assay was performed as described previously (Borecká-Melkusová and  
167 Bujdáková, 2008; Rosenberg, 1984). It uses a biphasic separation method to measure

168 cell surface hydrophobicity. In short, for each species tested, 4 ml of bacterial  
169 suspension ( $OD_{600} = 0.1$ ;  $OD_{initial}$ ) was placed into a class tube, overlaid with 1 ml of  
170 n-hexadecane (Sigma Aldrich), and vortexed for 3 min. The phases were then allowed  
171 to separate for 15 min, after which the ODs of the aqueous (lower) phase containing  
172 hydrophilic cells was measured at  $OD_{600}$  ( $OD_{residual}$ ). The hydrophobic cells are found  
173 in the n-hexadecane overlay (upper phase). OD values were compared to the bacterial  
174 suspension before mixing with n-hexadecane. The relative hydrophobicity (RH) was  
175 calculated as follows:  $RH = ((OD_{initial} - OD_{residual})/OD_{initial}) \times 100\%$ . The experiment  
176 was performed in triplicate with independent bacterial overnight cultures.

177

### 178 **Biofilm quantification by use of crystal violet (CV)**

179 Biofilm formation was assayed and quantified as previously described (Ren et al.,  
180 2015). Briefly, exponential growth phase cultures of the six species were adjusted to  
181 an optical density at 600nm ( $OD_{600}$ ) of 0.1 in R2A medium. Biofilm formation was  
182 assayed in a 96 well plate using eight replicates for each treatment. For single isolates  
183 an inoculation volume of 180  $\mu$ l was used and for the six-species biofilm 30  $\mu$ l per  
184 species. After 48 h of incubation at 18°C with shaking (200 r.p.m) biofilm formation  
185 was quantified by a modified crystal violet (CV) assay (Peeters et al., 2008).

186

### 187 **Characterizing nutrient utilisation**

188 To characterise the nutrient profiles (niches) of *Hydras* microbiota, we measured the  
189 carbon metabolism profile for each species using BIOLOG GN2 plates. BIOLOG  
190 GN2 plates are 96-well microwell plates containing 95 different carbon sources plus a  
191 carbon-absent water control well. Species were grown from isolate stocks in R2A  
192 medium (18°C, shaken at 250 r.p.m.), centrifuged at 3000 r.c.f. for 5 min, re-  
193 suspended in S medium and adjusted to an  $OD_{600}$  of 0.1. Each well of the BIOLOG  
194 plate was inoculated with 150  $\mu$ l of bacterial suspension and incubated for three days  
195 at 18°C in a humid chamber. Growth on each of the 95 nutrients was determined as  
196  $OD_{600}$  of each well using a TECAN plate reader. For each plate, the OD of the water  
197 control was subtracted from the reading of all other wells prior to analysis, and  
198 differenced OD values below 0.005 were considered as no growth (Vaz Jauri et al.,  
199 2013). Nutrient use was evaluated on three replicate plates. Nutrient (niche) overlap  
200 (NO) was calculated using the formula:  $NO = (\text{number of nutrients used by both A and B}) / ((\text{number of nutrients used by A} + \text{number of nutrients used by B}) / 2)$  (Vaz  
201 Jauri et al., 2013). A value of 1 indicates the use of the same nutrients (100% overlap)  
202 and 0 indicates no nutrient overlap among the 95 substrates tested. We also calculated  
203 the relative use of the eleven functional groups (carbohydrates, carboxylic acids,  
204 amino acids, polymers, aromatic chemicals, amines, amides, phosphorylated  
205 chemicals, esters, alcohols and bromide chemicals) according to Daou et al. (2017). In  
206 brief, the relative use of C substrates was calculated as absorption values in each well  
207 divided by the total absorption in the plate.

208

### 209 **Measurement of bacterial growth rates *in vitro***

210 Cultures of the all six species were produced in R2A microcosms (grown for 72 h at  
211 18°C, at 250 r.p.m). Aliquots of each culture were first washed in S medium and then  
212 re-suspended in fresh R2A medium to an optical density of 0.025 at 600 nm ( $OD_{600}$ ).  
213 Growth kinetics of all species were determined in 96-well microtiter plates. A 100  $\mu$ l  
214 aliquot of each re-suspension was pipetted into 100  $\mu$ l of fresh R2A medium. The  
215 microtiter plate was then placed in a microplate reader (TECAN Spark 10M, Tecan  
216 Group Ltd., Switzerland), and the  $OD_{600}$  of each well was measured at 30 min  
217

218 intervals for 96 cycles (with 10 sec shaking at 150 r.p.m. prior to each read). The  
219 growth of each species was determined in five well locations on an individual 96-well  
220 plate, which was replicated six times. The maximum growth rate ( $V_{\max}$ ) was  
221 calculated from the maximum slope of the absorbance over time.

222

### 223 **Statistical analysis**

224 Analysis of variance (ANOVA) and subsequent post hoc Tukey-Kramer tests were  
225 used to test for differences in the carrying capacity of the six *Hydra* colonizers. To  
226 meet the requirements for the model, the variable was Box-Cox transformed. A  
227 Welch ANOVA (and subsequent Wilcoxon posthoc tests) was used to test for  
228 differences in the fraction of the different species in the community, differences in  
229 biofilm formation capacity, and *in vitro* growth rates between the species.

230 Analysis of variance (ANOVA) and subsequent post hoc Tukey-Kramer tests were  
231 used to test for differences in the cell surface hydrophobicity of the six *Hydra*  
232 colonizers.

233 Sample size was chosen to maximise statistical power and ensure sufficient  
234 replication. Assumptions of the tests, that is, normality and equal distribution of  
235 variances, were visually evaluated. Non-significant interactions were removed from  
236 the models. Effects were considered significant at the level of  $P < 0.05$ . All statistical  
237 analyses were performed with JMP 9. Graphs were produced with GraphPad Prism  
238 5.0, and RStudio (RStudio Team, 2015).

239

## 240 **Results**

### 241 **Fundamental and realized niche occupation of the different bacterial species**

242 In mono-colonisations, the six bacterial species differ significantly in their carrying  
243 capacity on *Hydra* (Figure 1A; ANOVA:  $F_{5,12}=12.696$ ,  $P=0.0002$ ). The most extreme  
244 cases are *Acidovorax sp.* that reaches the highest numbers with  $2.6 \cdot 10^5$  CFUs/polyp,  
245 and *Duganella sp.* the lowest with  $1.7 \cdot 10^4$  CFUs/polyp. Based in the carrying  
246 capacity of the single species in mono-colonisations, we estimated the fundamental  
247 niche of each of the six species. The realized niche of the six bacterial species is  
248 calculated based on previously published data on the composition of the extremely  
249 stable microbial community. The species differed in their relative abundance as part  
250 of the microbial community (Figure 1B; Welch ANOVA:  $F_{5,14}=86.722$ ,  $P<0.0001$ ).  
251 The most dominant species is *Curvibacter sp.* representing 65% of the microbial  
252 community, followed by *Duganella sp.* that reaches about 16%. All other four species  
253 reach only comparatively low fractions (around 1%), with *Acidovorax sp.* being the  
254 lowest. When comparing the fundamental to the realized niche (Figure 2), we find  
255 that the realized niche of *Curvibacter sp.* and *Duganella sp.* is larger than their  
256 fundamental niche. This is in contrast to all other species, where as expected by  
257 theory, competition with other microbes leads to a smaller realized than the  
258 fundamental niche.

259

### 260 **Bacterial traits**

#### 261 *Associated with occupation of the fundamental niche*

262 The BATH assay was conducted with six species of the *Hydra* microbiome to  
263 measure cell surface hydrophobicity (CSH). The CSH of the bacterial species spanned  
264 a medium wide range; the values ranged from 0% to 42% and differs significantly  
265 between species (ANOVA:  $F_{5,12}=26.869$ ;  $P<0.0001$ ). *Curvibacter sp.* and *Pelomonas*  
266 *sp.* were the only two species that didn't show any affinity to the hexadecane; thus  
267 their cell population can be considered homogeneous consisting of only hydrophilic  
268 cells, which significantly differs from the others, except for *Pseudomonas sp.* (Figure  
269 3A). *Pseudomonas sp.* and *Undibacterium sp.* show a mixed cell population, where  
270 10 to 20% of the cells are hydrophobic. The species with the highest percentage of  
271 hydrophobic cells are *Acidovorax sp.* and *Duganella sp.*, between 30 and 35%.

272 The species differed in their biofilm formation (Welch ANOVA:  
273  $F_{5,18}=350.723$ ,  $P<0.0001$ ). All species formed biofilms (Figure 3B), with *Pelomonas*  
274 *sp.* producing the largest biomass amount, which significantly differed from all other  
275 species. The biofilm amount of *Acidovorax sp.* was also significantly different from  
276 all other species but only roughly a third of the mass that *Pelomonas sp.* produced. All  
277 other species didn't differ and are comparatively weak biofilm producers.

278 Nutrient utilisation of all species was determined using a BIOLOG assay. The  
279 94 carbon substrates are organized into eleven functional groups (Figure 4). Results  
280 showed that all six species actively oxidize carbon compounds such as carbohydrates  
281 (30-50% relative use), carboxylic acids (15-35% relative use) and amino acids (15-  
282 35% relative use) (Figure 4; Figure 5A). Carbohydrates are being used to an equal  
283 extent between all species, except for *Undibacterium sp.*, which uses the highest  
284 amount of around 50% (relative use). Turanose is the compound most highly utilised,  
285 followed by  $\alpha$ -D-lactose, L-rhamnose, and D-cellobiose. The use of carboxylic acids  
286 increases in the species, which are characterized by low frequencies in the *Hydra*  
287 microbiome, with the exception of *Duganella sp.* (with a relative use of 25-30%).  
288 Here D-galactonic acid lactone is the substrate with the highest usage, followed by  
289 different forms of hydroxyl butyric acids. Amino acids are most excessively used by

290 *Acidovorax sp.*, *Curvibacter sp.* and *Pseudomonas sp.*, whereas the other species use  
291 amino acids to a lesser extent. Polymers are being used very differently between the  
292 species with *Pseudomonas sp.* showing the highest and *Undibacterium sp.* the lowest  
293 values. Amines are being used more frequent by the dominant species in the  
294 microbiome and are utilized to a lesser extent by the low abundant species.

295

296 *Associated with occupation of the realized niche*

297 When comparing the *in vitro* growth rates we find species perform differently (Figure  
298 3C; Welch ANOVA:  $F_{5,174}=223.856$ ,  $P<0.0001$ ). The fastest species, *Undibacterium*  
299 *sp.*, grows twice as fast as compared to the slowest one, *Pelomonas sp.*.

300 The overlap in carbon substrate usage between all six microbiome members is  
301 displayed as a Venn diagram (Figure 5B). There are only two substrates, which are  
302 not utilized by any species, whereas 20 substrates are used by all species. There are  
303 only two species that can metabolize substrates that none of the other species is using.  
304 While *Pseudomonas sp.* uses two substrates: i-erythritol and lactulose, *Curvibacter*  
305 *sp.* is able to utilise eight substrates: D-arabitol, D-mannose, D-trehalose, mono-  
306 methyl succinate, formic acid, glucuronamide, L-pyroglutamic acid, and D-serine.  
307 The number of substrates shared exclusively between two species only is between one  
308 and two.

309 Niche overlap (NO) among all pairwise species combinations ranged from 60  
310 to 80% (Figure 5C). *Curvibacter sp.* shares the highest overlap (80%) with  
311 *Pseudomonas sp.* and *Duganella sp.*. For the other species the overlap ranges between  
312 60 and 70%. *Duganella sp.* displays the highest overlap with *Pseudomonas sp.* and  
313 *Undibacterium sp.* around 80%, whereas the overlap between *Pelomonas sp.* and  
314 *Acidovorax sp.* reaches almost 70%. *Undibacterium sp.* exhibits an overlap of 60 to  
315 70% with *Acidovorax sp.*, *Pseudomonas sp.* and *Pelomonas sp.*. *Acidovorax sp.* a  
316 80% overlap with *Pseudomonas sp.* and 70% overlap with *Pelomonas sp.*.  
317 *Pseudomonas sp.* and *Pelomonas sp.* show a 75% overlap of the nutrients used. Mean  
318 niche overlap was determined as the mean of all pairwise niche overlap values for  
319 each species. Comparing the number of nutrients being used by the individual species  
320 we find that *Curvibacter sp.* and *Pseudomonas sp.* are able to use 70% of the provided  
321 substrates. *Duganella sp.* uses 57%, *Acidovorax sp.* 54% and *Pelomonas sp.* 51%.  
322 The lowest substrate utilization was measured for *Undibacterium sp.* with 41% of the  
323 available substrates.

324 Overall, we find that neither the occupation of the fundamental or the realized  
325 niche can be linked to a specific bacterial trait or substrate utilization pattern (Figure  
326 6).

327



## 328 **Discussion**

329 Microbial communities residing in abiotic environments typically comprise numerous  
330 interacting species. Such communities have been studied with traditional approaches,  
331 for example the niche-assembly concept, which is an extension of the classical niche  
332 theory (Hutchinson, 1957). The niche-assembly perspective proposes that any  
333 ecosystem is made up of a limited number of niches, each occupied by a single  
334 species (Wennekes et al., 2012). Thus, the partitioning of these niches leads to the  
335 stable coexistence of competing species within an ecosystem. To assess the rules of  
336 assembly and coexistence of microbiota in host-associated microbiomes, we here  
337 apply the niche-assembly perspective to a metaorganism, and thus specifically extend  
338 the concept to biotic environments.

339 We find that the fundamental niche (here defined by the absence of  
340 interspecific microbial interactions) differs considerably from the realized niche of  
341 *Hydras* associated microbes (Figure 2). This reflects the difference in performance  
342 between the species when they individually occupy *Hydra* (mono-association) as to  
343 when they occur as part of their microbial community on the host. As predicted by  
344 niche theory, we find for the majority of the species that the realized niche is smaller  
345 than the fundamental one, most likely caused by interspecific microbial competition,  
346 as has also been observed in other systems, e.g. *Vibrios* in their marine environment  
347 (Materna et al., 2012). In our study, the best colonizer in the mono-colonisations,  
348 *Acidovorax sp.* (as also observed by Fraune et al. (2015)), is the least abundant  
349 species as part of the microbial community. This is different for the two main  
350 colonizers in the community, *Curvibacter sp.* and *Duganella sp.*, where the realized  
351 niche is six times the size of the fundamental niche for *Curvibacter sp.*, and about ten  
352 times the size for *Duganella sp.*. This finding is very interesting and indicates that the  
353 two species benefit from interactions when part of the microbiome. This can happen  
354 directly through positive interactions with the other members of the microbiome or  
355 indirectly by benefitting from the interactions between the other microbiome  
356 members and the host. We draw attention to the fact that the latter aspect differs from  
357 the classical Hutchinson niche concept, in that in our case the environment, i.e. the  
358 host, has the potential to change its interactions depending on the specific bacterial  
359 colonizers. Our finding also highlights the importance of the low frequency  
360 community members in shaping the overall community composition, as has recently  
361 been suggested for *Hydra* (Deines et al., 2020).

362 For linking the community composition in *Hydra*'s microbiome to specific  
363 characteristics, we used a trait-based approach focussing on traits potentially involved  
364 in microbiome assembly and stability. A first step in microbiome assembly is the  
365 attachment to host surfaces, which can happen in a multitude of ways. In the human  
366 intestine, for example, microbes have been found to bind to mucin, a major  
367 component of the human mucosa (de Vos, 2015). Adhesion is thus thought to be a  
368 powerful mechanism for exerting both, positive and negative selection for or against  
369 specific microbes (McLoughlin et al., 2016; Schluter et al., 2015). Amongst others  
370 (van Loosdrecht et al., 1987), bacterial cell surface hydrophobicity has been shown to  
371 play a crucial role in surface attachment (Krasowska and Sigler, 2014). In general,  
372 hydrophobic cells adhere more strongly to hydrophobic surfaces and vice versa  
373 (Giaouris et al., 2009; Kochkodan et al., 2008). Nevertheless, the heterogeneity of a  
374 bacterial population needs to be taken into account. For example, the presence of  
375 both, hydrophilic and hydrophobic cells, have been observed in planktonic bacteria  
376 cell populations, implying that only part of the population participates in an adhesion  
377 process to substrates (Krasowska and Sigler, 2014). We also observe mixed cell

378 populations for most of *Hydra* microbial associates, except for two species,  
379 *Curvibacter sp.* and *Pelomonas sp.*, which only consist of hydrophobic cells. They  
380 seem to be perfectly adapted to *Hydras* epithelial cells, which are coated with a  
381 carbohydrate-rich layer, the glycocalyx (Ouwerkerk et al., 2013; Schröder and Bosch,  
382 2016). The microbiome inhabits the outer mucus-like layer of the glycocalyx (Fraune  
383 et al., 2015), which is hydrophilic. Thus, hydrophilic bacterial cells should adhere  
384 more strongly to *Hydra* than hydrophobic cells. Both, *Curvibacter sp.* and *Pelomonas*  
385 *sp.*, have been shown to be of particular importance to the host. *Curvibacter sp.* shows  
386 signs of coevolution with its host and contributes to fungal resistance against the  
387 filamentous fungus *Fusarium* (Fraune et al., 2015). *Pelomonas sp.* has been shown to  
388 be of central importance in modulating the spontaneous body contractions in *Hydra*  
389 (Murillo-Rincon et al., 2017). So both species contribute to host fitness, providing the  
390 opportunity for the speculation that the host actively selects for specific microbes.  
391 This could happen, for example, by controlling the production and release of adhesive  
392 molecules from the host epithelium as suggested by (McLoughlin et al., 2016).

393 After successful attachment, bacteria need to colonise the habitat. In most  
394 cases, this happens through the formation of biofilms, as has been reported for the gut  
395 (de Vos, 2015; Kania et al., 2007). The biofilm succeeds the planktonic phase in the  
396 bacterial life cycle (McDougald et al., 2012) and represents a key ecological process  
397 for the colonization of different habitats. Thus, the difference in the ability to form  
398 biofilms could provide an explanation for why one species outcompetes the other  
399 species or has got a higher chance of persistence in the *Hydra* ecosystem. Further,  
400 biofilms have been shown to protect bacterial cells from various environmental  
401 stressors (Flemming and Wingender, 2010). Interestingly, from the six species tested  
402 here, the one with the highest ability to form biofilms is *Pelomonas sp.*, whereas the  
403 two main colonizers, *Curvibacter sp.* and *Duganella sp.* show a reduced capacity to  
404 form biofilms. Our finding indicates that the capability of biofilm formation is not a  
405 good predictor of the bacterial performance in the *Hydra* habitat. Nevertheless, it  
406 might be of importance for the establishment and persistence of some of the low  
407 abundance species, such as *Pelomonas sp.* and *Acidovorax sp.*.

408 Importantly, microbiomes on external surfaces of metaorganisms, such as the  
409 skin, have been reported to be highly stable despite their constant exposure to  
410 extrinsic factors (Oh et al., 2016). Whereas bacterial diversity is widely recognized in  
411 leading to temporal stability of ecosystem processes (Bell et al., 2009; Griffin et al.,  
412 2009; Prosser et al., 2007), the influence of resource niche breadth has received little  
413 scientific attention (Hunting et al., 2015). Recent work studying the decomposition of  
414 organic matter in experimental microcosms found that the higher the overlap in  
415 resource niches, the higher the stability of the microbial community. It is reasonable  
416 to assume that the same underlying principles govern stability in host-associated  
417 microbial communities. We therefore measured the niche overlap and resource use of  
418 the six species isolated from the *Hydra* microbiome. Interestingly, we find the niche  
419 overlap between all pairwise combinations to be between 60 and 80%, with about  
420 20% of the carbon sources being metabolized by all species. This suggests that  
421 metabolic overlap could be involved in promoting the extreme temporal stability of  
422 *Hydra's* microbiome (Fraune and Bosch, 2007). We also found the two main  
423 colonisers, *Curvibacter sp.* and *Duganella sp.*, to possess the widest resource niche  
424 breadth of all species, and that five out of six species were able to metabolize more  
425 than 50% of the 95 offered carbon substrates. Overall, the relative niche breadth  
426 observed in the tested species can serve as a proxy of the metabolic diversity of the  
427 *Hydra* microbiome.

428           The metabolic overlap, i.e. redundancy, within *Hydra*'s microbial community  
429 indicates that the individual species are not occupying a specific metabolic niche.  
430 Nevertheless, the only one for which we observed a specific carbon usage pattern is  
431 the main colonizer *Curvibacter sp.*, which utilizes eight carbon sources that are not  
432 metabolized by any other tested microbiome members. Whether this hints at the  
433 occupation of a specific niche within *Hydra*'s microbial community and can be linked  
434 to the observation that its realized is bigger than its fundamental niche when part of  
435 the community as compared to single occupation on *Hydra*, is currently open to  
436 speculation. An alternative option might be that *Curvibacter sp.* is auxotrophic in  
437 producing certain amino acids, as are 98% of all sequenced microbes (Zengler and  
438 Zaramela, 2018), and thus relies on the uptake of external substrates that might not be  
439 secreted by the host but by its fellow community members. Analysing the metabolic  
440 interactions within this microbial network will be essential for understanding  
441 community assembly, composition, and maintenance.

442           In summary we find that the here measured bacterial traits vary across  
443 microbiome members. Further, the dominant species in the microbiome do not  
444 necessarily perform best in all of the measured traits. We rather observe that all  
445 species, independent of their density, perform well in a subset of traits, likely  
446 facilitating the coexistence of several niches within the host ecosystem. Whether a  
447 change in the realized niche of microbes can be linked to potential for dysbiosis is an  
448 interesting aspect, which warrants further investigation.  
449

450 **Ethics statement**

451 Ethical restrictions do not apply to cnidarian model organisms such as *Hydra*.

452

453 **Author contributions**

454 PD and KH designed the experiments. PD performed the experiments. PD and KH  
455 analysed the data. PD, KH and TB wrote the paper.

456

457 **Funding**

458 PD received funding from the European Union's Framework Programme for  
459 Research and Innovation Horizon 2020 (2014–2020) under the Marie Skłodowska-  
460 Curie Grant Agreement No. 655914 and KH under the Marie Skłodowska-Curie  
461 Grant Agreement No. 657096. Both also received a Reintegration Grant from the  
462 Deutscher Akademischer Austausch Dienst (DAAD). This work was further  
463 supported by the Deutsche Forschungsgemeinschaft (DFG) Collaborative Research  
464 Centre (CRC) 1182 (“Origin and Function of Metaorganisms”).

465

466 **Acknowledgements**

467 TB gratefully appreciates support from the Canadian Institute for Advanced Research  
468 (CIFAR) and thanks the Wissenschaftskolleg (Institute of Advanced Studies) in  
469 Berlin for a sabbatical leave.

470

471 **Competing Interests**

472 The authors declare no conflict of interest.

473

474 **References**

- 475 Bell, T., Gessner, M. O., Griffiths, R. I., McLaren, J. R., Morin, P. J., and van der  
476 Heijden, M. (2009). “Microbial diversity and ecosystem functioning under  
477 controlled conditions and in the wild,” in *Biodiversity, Ecosystem Functioning,  
478 and Human Wellbeing*, eds. S. Naeem, D. E. Bunker, A. Hector, M. Loreau, and  
479 C. P. Perring (Oxford, UK), 121–133.
- 480 Borecká-Melkusová, S., and Bujdáková, H. (2008). Variation of cell surface  
481 hydrophobicity and biofilm formation among genotypes of *Candida albicans* and  
482 *Candida dubliniensis* under antifungal treatment. *Can.J. Microbiol.* 54, 718–724.  
483 doi:10.1139/w08-060.
- 484 Bosch, T. C. G. (2013). Cnidarian-microbe interactions and the origin of innate  
485 immunity in metazoans. *Annu. Rev. Microbiol.* 67, 499–518.  
486 doi:10.1146/annurev-micro-092412-155626.
- 487 Daou, L., Luglia, M., Périsol, C., Calvert, V., and Criquet, S. (2017). Sporulation and  
488 physiological profiles of bacterial communities of three Mediterranean soils  
489 affected by drying-rewetting or freezing-thawing cycles. *Soil Biol. Biochem.* 113,  
490 116–121. doi:10.1016/j.soilbio.2017.06.008.
- 491 de Vos, W. M. (2015). Microbial biofilms and the human intestinal microbiome. *NPJ*  
492 *Biofilms Microbiomes* 1, 15005. doi:10.1038/npjbiofilms.2015.5.
- 493 Deines, P., and Bosch, T. C. G. (2016). Transitioning from microbiome composition  
494 to microbial community interactions: the potential of the metaorganism *Hydra* as  
495 an experimental model. *Front. Microbiol.* 7, 1610.  
496 doi:10.3389/fmicb.2016.01610.
- 497 Deines, P., Hammerschmidt, K., Bosch, T. C. B. (2020). Microbial species  
498 coexistence depends on the host environment. *bioRxiv*  
499 <https://doi.org/10.1101/609271>
- 500 Deines, P., Lachnit, T., and Bosch, T. C. G. (2017). Competing forces maintain the  
501 *Hydra* metaorganism. *Immunol. Rev.* 279, 123–136. doi:10.1111/imr.12564.
- 502 Falkowski, P. G., Fenchel, T., and DeLong, E. F. (2008). The microbial engines that  
503 drive Earth's biogeochemical cycles. *Science* 320, 1034–1039.  
504 doi:10.1126/science.1153213.
- 505 Flemming, H. C., and Wingender, J. (2010). The biofilm matrix. *Nat. Rev. Microbiol.*  
506 8, 623–633. doi:10.1038/nrmicro2415.
- 507 Franzenburg, S., Walter, J., Künzel, S., Wang, J., Baines, J. F., Bosch, T. C. G., et al.  
508 (2013). Distinct antimicrobial peptide expression determines host species-specific  
509 bacterial associations. *Proc. Natl. Acad. Sci. U.S.A.* 110, E3730–8.  
510 doi:10.1073/pnas.1304960110.
- 511 Fraune, S., and Bosch, T. C. G. (2007). Long-term maintenance of species-specific  
512 bacterial microbiota in the basal metazoan *Hydra*. *Proc. Natl. Acad. Sci. U.S.A.*  
513 104, 13146–13151. doi:10.1063/1.1599624.

- 514 Fraune, S., Anton-Erxleben, F., Augustin, R., Franzenburg, S., Knop, M., Schröder,  
515 K., et al. (2015). Bacteria-bacteria interactions within the microbiota of the  
516 ancestral metazoan *Hydra* contribute to fungal resistance. *ISME J.* 9, 1543–1556.  
517 doi:10.1038/ismej.2014.239.
- 518 Giaouris, E., Chapot-Chartier, M.-P., and Briandet, R. (2009). Surface  
519 physicochemical analysis of natural *Lactococcus lactis* strains reveals the  
520 existence of hydrophobic and low charged strains with altered adhesive  
521 properties. *Int. J. Food Microbiol.* 131, 2–9.  
522 doi:10.1016/j.ijfoodmicro.2008.09.006.
- 523 Green, J. L., Bohannan, B. J. M., and Whitaker, R. J. (2008). Microbial biogeography:  
524 from taxonomy to traits. *Science* 320, 1039–1043. doi:10.1126/science.1153475.
- 525 Griffin, J. N., O’Gorman, E. J., Emmerson, M. C., Jenkins, S. R., Klein, A. M., and  
526 Loreau, M. (2009). “Biodiversity and the stability of ecosystem functioning,” in  
527 *Biodiversity, Ecosystem Functioning, and Human Wellbeing*, eds. S. Naeem, D.  
528 E. Bunker, A. Hector, M. Loreau, and C. P. Perring (Oxford, UK: Oxford  
529 University Press), 78–93.
- 530 Guittar, J., Shade, A., and Litchman, E. (2019). Trait-based community assembly and  
531 succession of the infant gut microbiome. *Nat. Commun.* 10, 512.  
532 doi:10.1038/s41467-019-08377-w.
- 533 Holt, R. D. (2009). Bringing the Hutchinsonian niche into the 21st century: ecological  
534 and evolutionary perspectives. *Proc. Natl. Acad. Sci. U.S.A.* 106, 19659–19665.  
535 doi:10.1073/pnas.0905137106.
- 536 Hunting, E. R., Vijver, M. G., van der Geest, H. G., Mulder, C., Kraak, M. H. S.,  
537 Breure, A. M., et al. (2015). Resource niche overlap promotes stability of  
538 bacterial community metabolism in experimental microcosms. *Front. Microbiol.*  
539 6, 11512. doi:10.3389/fmicb.2015.00105.
- 540 Hutchinson, G. E. (1957). Concluding remarks. *Cold Spring Harb. Sym.* 22, 415–427.
- 541 Kania, R. E., Lamers, G. E. M., Vonk, M. J., Huy, P. T. B., Hiemstra, P. S.,  
542 Bloemberg, G. V., et al. (2007). Demonstration of bacterial cells and glycocalyx  
543 in biofilms on human tonsils. *Arch. Otolaryngol.* 133, 115–121.  
544 doi:10.1001/archotol.133.2.115.
- 545 Kau, A. L., Ahern, P. P., Griffin, N. W., Goodman, A. L., and Gordon, J. I. (2011).  
546 Human nutrition, the gut microbiome and the immune system. *Nature* 474, 327–  
547 336. doi:10.1038/nature10213.
- 548 Kochkodan, V., Tsarenko, S., Potapchenko, N., Kosinova, V., and Goncharuk, V.  
549 (2008). Adhesion of microorganisms to polymer membranes: a photobactericidal  
550 effect of surface treatment with TiO<sub>2</sub>. *Desalination* 220, 380–385.  
551 doi:10.1016/j.desal.2007.01.042.
- 552 Kopac, S. M., and Klassen, J. L. (2016). Can they make it on their own? Hosts,  
553 microbes, and the holobiont niche. *Front. Microbiol.* 7, 1647.  
554 doi:10.3389/fmicb.2016.01647.

- 555 Krasowska, A., and Sigler, K. (2014). How microorganisms use hydrophobicity and  
556 what does this mean for human needs? *Front. Cell. Infect. Microbiol.* 4, 653.  
557 doi:10.3389/fcimb.2014.00112.
- 558 Krause, S., Le Roux, X., Niklaus, P. A., Van Bodegom, P. M., Lennon, J. T.,  
559 Bertilsson, S., et al. (2014). Trait-based approaches for understanding microbial  
560 biodiversity and ecosystem functioning. *Front. Microbiol.* 5, 2019.  
561 doi:10.3389/fmicb.2014.00251.
- 562 Leibold, M. A. (1995). The niche concept revisited: mechanistic models and  
563 community context. *Ecology* 76, 1371–1382. doi:10.2307/1938141.
- 564 Lenhoff, H. M., and Brown, R. D. (1970). Mass culture of *Hydra*: an improved  
565 method and its application to other aquatic invertebrates. *Lab. Anim.* 4, 139–154.  
566 doi:10.1258/00236770781036463.
- 567 Louca, S., Polz, M. F., Mazel, F., Albright, M. B. N., Huber, J. A., O'Connor, M. I.,  
568 et al. (2018). Function and functional redundancy in microbial systems. *Nat. Ecol.*  
569 *Evol.* 2, 936–943. doi:10.1038/s41559-018-0519-1.
- 570 Martiny, J. B. H., Jones, S. E., Lennon, J. T., and Martiny, A. C. (2015). Microbiomes  
571 in light of traits: a phylogenetic perspective. *Science* 350, aac9323–aac9323.  
572 doi:10.1126/science.aac9323.
- 573 Materna, A. C., Friedman, J., Bauer, C., David, C., Chen, S., Huang, I. B., et al.  
574 (2012). Shape and evolution of the fundamental niche in marine *Vibrio*. *ISME J.*  
575 6, 2168–2177. doi:10.1038/ismej.2012.65.
- 576 McDougald, D., Rice, S. A., Barraud, N., Steinberg, P. D., and Kjelleberg, S. (2012).  
577 Should we stay or should we go: mechanisms and ecological consequences for  
578 biofilm dispersal. *Nat. Rev. Microbiol.* 10, 39–50. doi:10.1038/nrmicro2695.
- 579 McFall-Ngai, M., Hadfield, M. G., Bosch, T. C. G., Carey, H. V., Domazet-Loso, T.,  
580 Douglas, A. E., et al. (2013). Animals in a bacterial world, a new imperative for  
581 the life sciences. *Proc. Natl. Acad. Sci. U.S.A.* 110, 3229–3236.  
582 doi:10.1073/pnas.1218525110.
- 583 McLoughlin, K., Schluter, J., Rakoff-Nahoum, S., Smith, A. L., and Foster, K. R.  
584 (2016). Host selection of microbiota via differential adhesion. *Cell Host Microbe*  
585 19, 550–559. doi:10.1016/j.chom.2016.02.021.
- 586 Murillo-Rincon, A. P., Klimovich, A., Pemöller, E., Taubenheim, J., Mortzfeld, B.,  
587 Augustin, R., et al. (2017). Spontaneous body contractions are modulated by the  
588 microbiome of *Hydra*. *Sci. Rep.* 7, 15937. doi:10.1038/s41598-017-16191-x.
- 589 Oh, J., Byrd, A. L., Park, M., NISC Comparative Sequencing Program, Kong, H. H.,  
590 and Segre, J. A. (2016). Temporal stability of the human skin microbiome. *Cell*  
591 165, 854–866. doi:10.1016/j.cell.2016.04.008.
- 592 Ouwerkerk, J. P., de Vos, W. M., and Belzer, C. (2013). Glycobiome: bacteria and  
593 mucus at the epithelial interface. *Best Pract. Res. Cl. Ga.* 27, 25–38.  
594 doi:10.1016/j.bpg.2013.03.001.

- 595 Pearman, P. B., Guisan, A., Broennimann, O., and Randin, C. F. (2008). Niche  
596 dynamics in space and time. *Trends Ecol. Evol.* 23, 149–158.  
597 doi:10.1016/j.tree.2007.11.005.
- 598 Peeters, E., Nelis, H. J., and Coenye, T. (2008). Comparison of multiple methods for  
599 quantification of microbial biofilms grown in microtiter plates. *J. Microbiol.*  
600 *Meth.* 72, 157–165. doi:10.1016/j.mimet.2007.11.010.
- 601 Pocheville, A. (2015). “The ecological niche: history and recent controversies,” in  
602 *Handbook of Evolutionary Thinking in the Sciences*, eds. T. Heams, P. Huneman,  
603 G. Lecointre, and M. Silberstein (Dordrecht: Springer, Dordrecht), 547–586.  
604 doi:10.1007/978-94-017-9014-7\_26.
- 605 Prosser, J. I., Bohannan, B. J. M., Curtis, T. P., Ellis, R. J., Firestone, M. K.,  
606 Freckleton, R. P., et al. (2007). The role of ecological theory in microbial  
607 ecology. *Nat. Rev. Microbiol.* 5, 384–392. doi:10.1038/nrmicro1643.
- 608 Ren, D., Madsen, J. S., Sørensen, S. J., and Burmølle, M. (2015). High prevalence of  
609 biofilm synergy among bacterial soil isolates in cocultures indicates bacterial  
610 interspecific cooperation. *ISME J.* 9, 81–89. doi:10.1038/ismej.2014.96.
- 611 Rosenberg, M. (1984). Bacterial adherence to hydrocarbons: a useful technique for  
612 studying cell surface hydrophobicity. *FEMS Microbiol Lett* 22, 289–295.  
613 doi:10.1111/j.1574-6968.1984.tb00743.
- 614 RStudio Team (2015). *RStudio: Integrated Development for R* (RStudio, Inc., Boston,  
615 MA). Available at: Available at <https://www.rstudio.com>.
- 616 Schluter, J., Nadell, C. D., Bassler, B. L., and Foster, K. R. (2015). Adhesion as a  
617 weapon in microbial competition. *ISME J.* 9, 139–149.  
618 doi:10.1038/ismej.2014.174.
- 619 Schröder, K., and Bosch, T. C. G. (2016). The origin of mucosal immunity: lessons  
620 from the holobiont *Hydra*. *mBio* 7, e01184–16. doi:10.1128/mBio.01184-16.
- 621 van Loosdrecht, M. C., Lyklema, J., Norde, W., Schraa, G., and Zehnder, A. J.  
622 (1987). The role of bacterial cell wall hydrophobicity in adhesion. *Appl. Environ.*  
623 *Microb.* 53, 1893–1897.
- 624 Vaz Jauri, P., Bakker, M. G., Salomon, C. E., and Kinkel, L. L. (2013). Subinhibitory  
625 antibiotic concentrations mediate nutrient use and competition among soil  
626 streptomyces. *PLoS ONE* 8, e81064. doi:10.1371/journal.pone.0081064.
- 627 Wein, T., Dagan, T., Fraune, S., Bosch, T. C. G., Reusch, T. B. H., and Hülter, N. F.  
628 (2018). Carrying capacity and colonization dynamics of *Curvibacter* in the *Hydra*  
629 host habitat. *Front. Microbiol.* 9, 185. doi:10.3389/fmicb.2018.00443.
- 630 Wenekes, P. L., Rosindell, J., and Etienne, R. S. (2012). The neutral-niche debate: a  
631 philosophical perspective. *Acta Biotheor.* 60, 257–271. doi:10.1007/s10441-012-  
632 9144-6.
- 633 Whittaker, R. H., Levin, S. A., and Root, R. B. (1973). Niche, habitat, and ecotope.



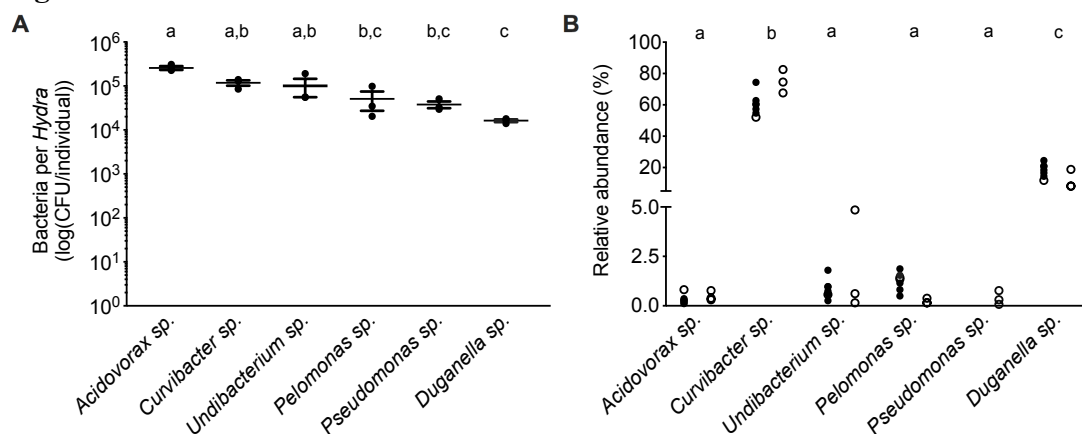
634 *Am. Nat.* 107, 321–338. doi:10.1086/282837;subPage:string:Access.

635 Zengler, K., and Zaramela, L. S. (2018). The social network of microorganisms - how  
636 auxotrophies shape complex communities. *Nat. Rev. Microbiol.* 16, 383–390.  
637 doi:10.1038/s41579-018-0004-5.

638

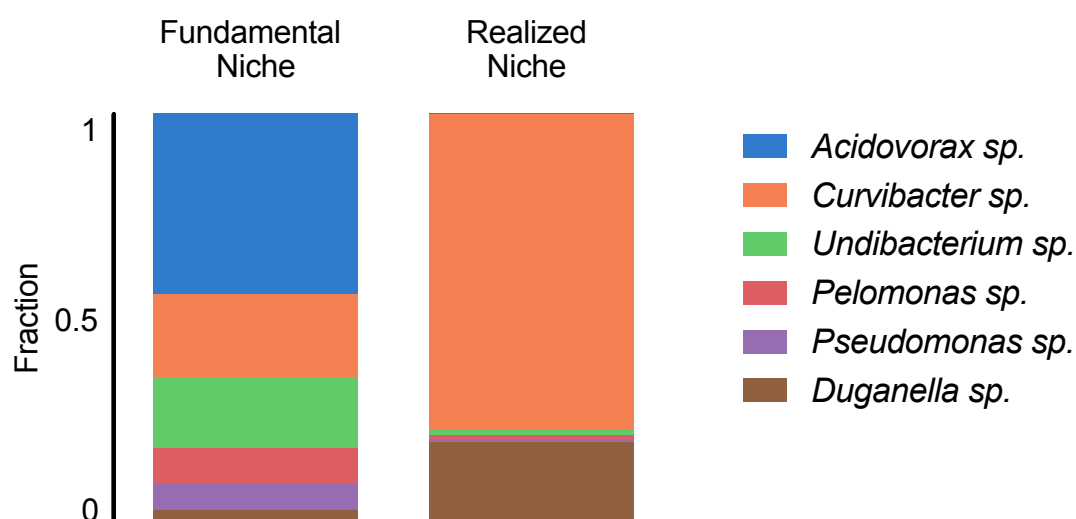
639

640 **Figures**

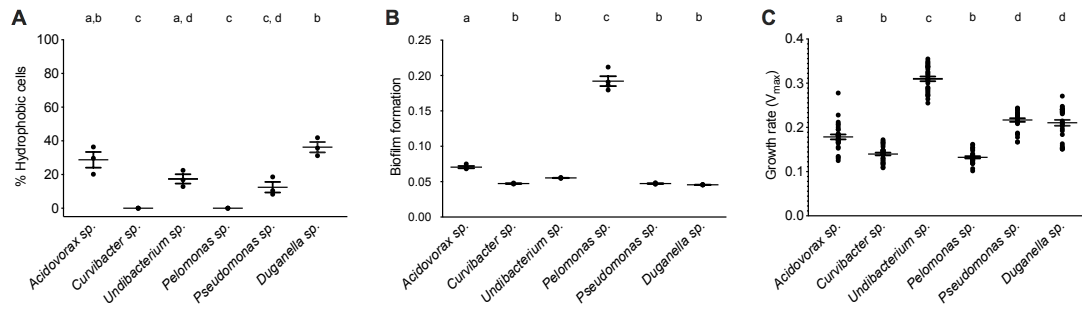


641  
 642 **Figure 1.** Performance of the six main bacterial colonizers isolated from the *Hydra*  
 643 microbiome. (A) Carrying capacity of the *Hydra* ecosystem during mono-associations  
 644 of germ-free polyps with individual bacterial species. Error bars are s.e.m., based on  
 645 n=3. (B) Relative abundances of the different bacterial colonizers in wild-type (open  
 646 circles) and conventionalized polyps (filled circles), compiled from previously  
 647 published studies (left: (Murillo-Rincon et al., 2017), right: (Franzenburg et al.,  
 648 2013)).

649  
 650  
 651  
 652



653  
 654 **Figure 2.** *Hydra* functions as an ecosystem, which allows for the niche allocation.  
 655 Shown are the fundamental and realized niches of six microbiome members (based on  
 656 mono-colonisations and microbial community composition). The realized niche  
 657 includes additional constrains arising from inter-specific competition between  
 658 microbiome members.



659

660

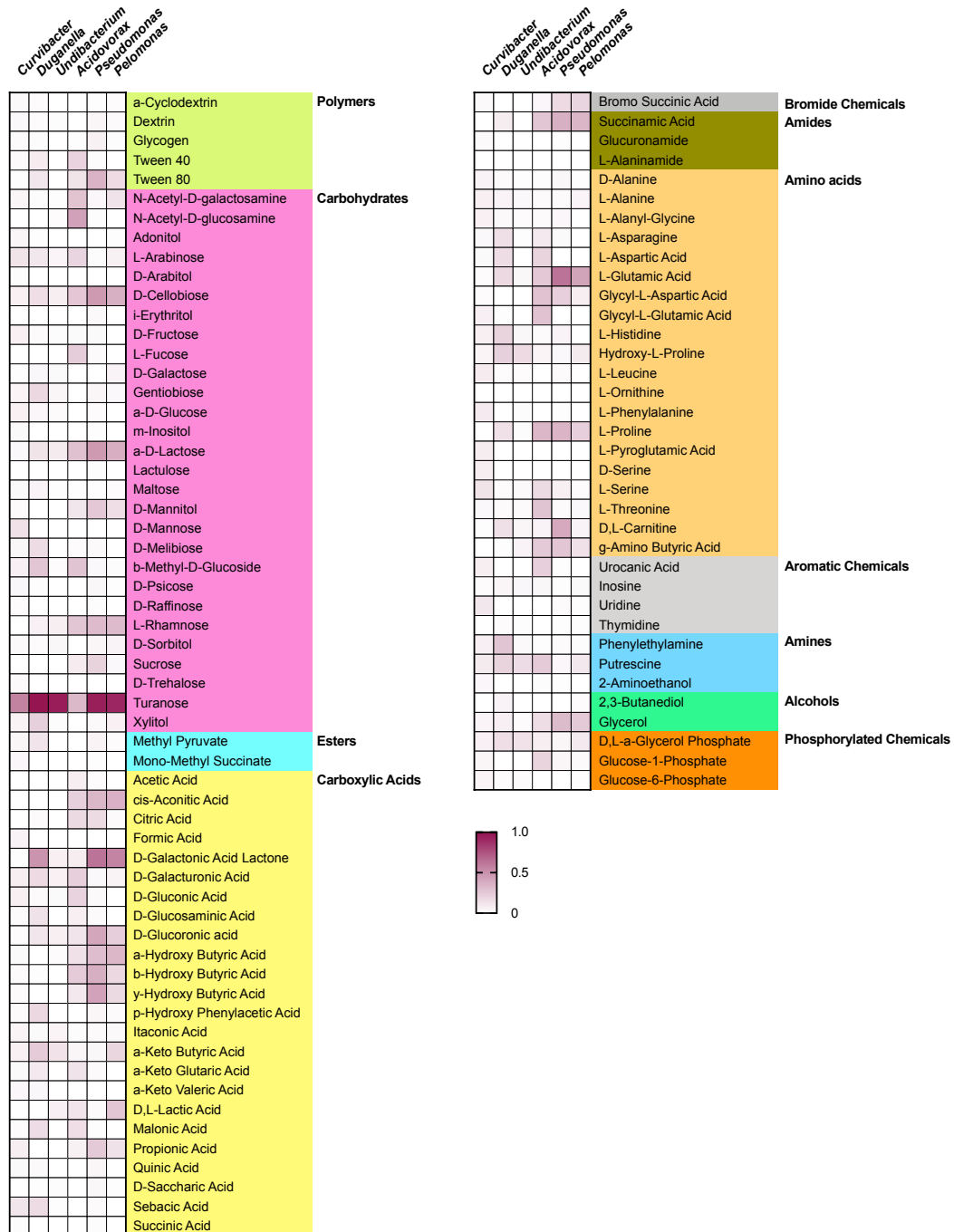
661 **Figure 3.** Trait measures of bacterial species isolated from the *Hydra* microbiome.

662 (A) Cell surface hydrophobicity (Error bars are s.e.m., n=3), and (B) Biofilm

663 formation capacity of six bacterial isolates. Error bars are s.e.m., n=4. (C) Bacterial

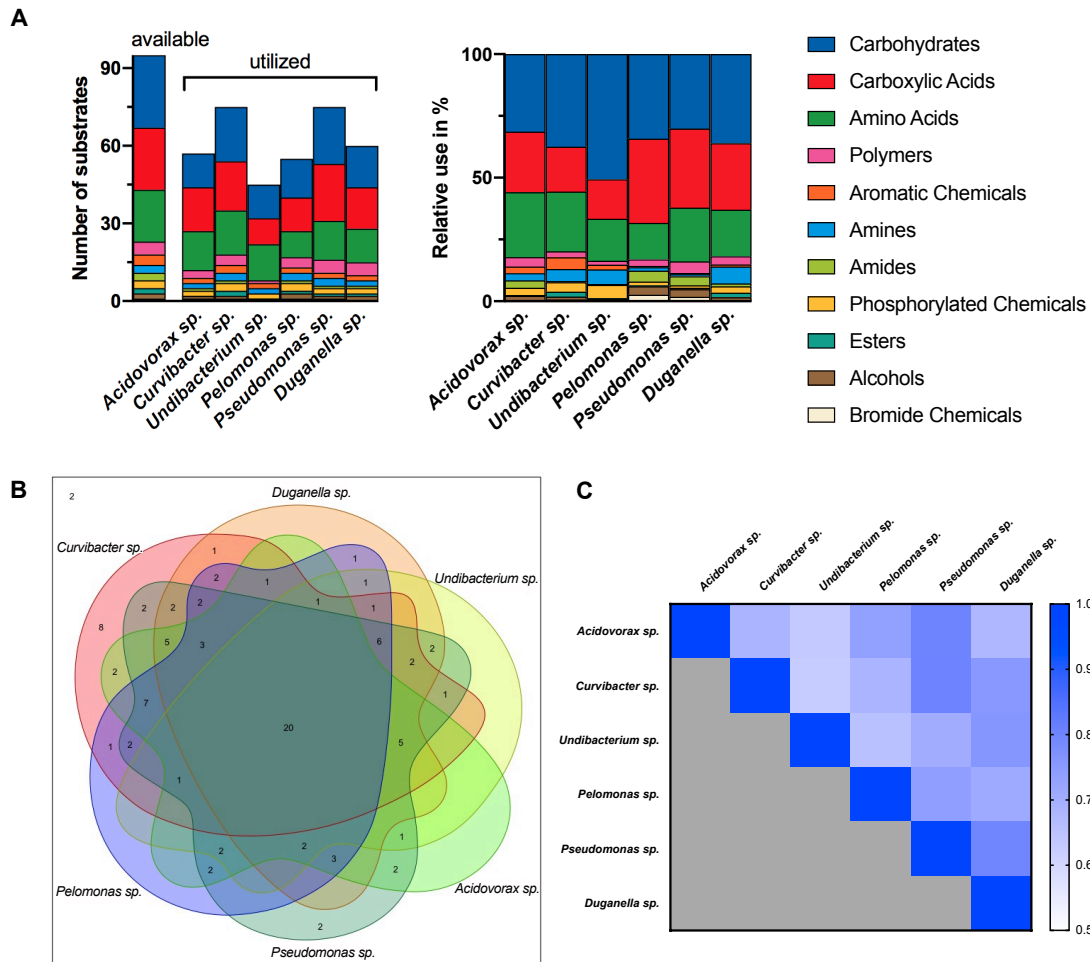
664 growth rates of individual species measured *in vitro*. Error bars are s.e.m., based on

664 n=30.



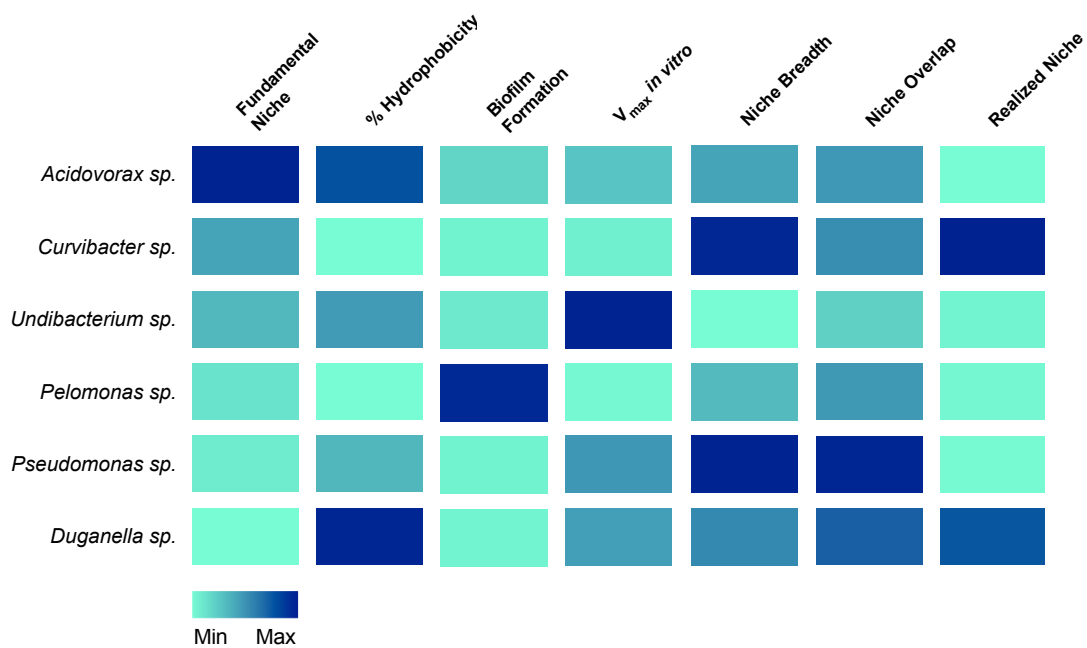
665  
666  
667  
668

**Figure 4.** Substrate utilization pattern of six bacterial isolates from the *Hydra* microbiome measured with a BIOLOG assay. Colours indicate the relative magnitude of substrate utilization.



669  
670  
671  
672  
673  
674  
675  
676

**Figure 5.** Metabolic similarity between *Hydra*'s microbiome members. **(A)** Number of substrates utilized and their relative use (%). **(B)** Venn diagram showing the distribution of shared substrates among the microbiome members. **(C)** Niche overlap among all pairwise combinations of six *Hydra* microbiome members. A value of 1 indicates the use of the same nutrients (100% overlap) and 0 indicates no nutrient overlap.



677  
678  
679  
680

**Figure 6.** Association of traits with the occupation of the fundamental and realized niches in *Hydra*'s six microbiome members.